

Selective zircon accumulation in a new benthic foraminifer, *Psammophaga zirconia*, sp. nov.

A. SABBATINI,¹ A. NEGRI,¹ A. BARTOLINI,² C. MORIGI,³ O. BOUDOUMA,⁴ E. DINELLI,⁵ F. FLORINDO,⁶ R. GALEAZZI,¹ M. HOLZMANN,⁷ P. C. LURCOCK,⁶ L. MASSACCESI,¹ J. PAWLOWSKI⁷ AND S. ROCCHI³

¹Dipartimento di Scienze della Vita e dell'Ambiente Di.S.V.A., Università Politecnica delle Marche, Ancona, Italy

²Centre de Recherche sur la Paléobiodiversité et les Paléoenvironnements, UMR 7207 CNRS MNHN UPMC, Muséum National d'Histoire Naturelle, Paris Cedex 05, France

³Dipartimento di Scienze della Terra, Università di Pisa, Pisa, Italy

⁴ISTEP (UMR 7193), Université Pierre et Marie Curie, Paris Cedex 05, France

⁵Dipartimento di Scienze Biologiche, Geologiche e Ambientali, Università di Bologna, Bologna, Italy

⁶Istituto Nazionale di Geofisica e Vulcanologia (INGV), Roma, Italy

⁷Department of Genetics and Evolution, Université de Genève, Geneva 4, Switzerland

ABSTRACT

Benthic foraminifera are single-celled eukaryotes that make a protective organic, agglutinated or calcareous test. Some agglutinated, single-chambered taxa, including *Psammophaga* Arnold, 1982, retain mineral particles in their cytoplasm, but the selective mechanism of accumulation is not clear. Here, we report the ability of a foraminiferal species to select and accumulate zircons and other heavy minerals in their cytoplasm. In particular, the use of Scanning Electron Microscope coupled with an Energy Dispersive X-ray microanalysis system (SEM–EDS) enabled a representative overview of the mineral diversity and showed that the analysed *Psammophaga zirconia* sp. nov. individuals contained dominantly crystals of zircon (51%), titanium oxides (27%), and ilmenite (11%) along with minor magnetite and other minerals. The studied specimens occur in the shallow central Adriatic Sea where the sediment has a content of zircon below 1% and of other heavy minerals below 4%. For that reason we hypothesize that: (i) *P. zirconia* may be able to chemically select minerals, specifically zircon and rutile; (ii) the chemical mechanism allowing the selection is based on electrostatic interaction, and it could work also for agglutinated foraminifera (whether for ingestion, like Xenophyophores, or incorporation in the test as in many other described taxa). In particular, this aptitude for high preferential uptake and differential ingestion or retention of zircon is reported here for the first time, together with the selection of other heavy minerals already described in members of the genus *Psammophaga*. They are generally counted among early foraminifera, constructing a morphologically simple test with a single chamber. Our molecular phylogenetic study confirms that *P. zirconia* is a new species, genetically distinctive from other *Psammophaga*, and occurs in the Adriatic as well as in the Black Sea.

Received 20 May 2015; accepted 18 January 2016

Corresponding author: A. Sabbatini. Tel.: +39 0712204329; fax: +39 0712204650; e-mail: a.sabbatini@univpm.it

INTRODUCTION

The ability of monothalamous (single-chambered) foraminifera, including *Psammophaga*, to selectively incorporate mineral grains into their cytoplasm has been known for some decades (Arnold, 1982; Pawlowski & Majewski, 2011; Balloero *et al.*, 2013). The etymology of the name *Psammophaga*

reflects the ingestion of sediment grains, which are retained in the cytoplasm as inclusions. Traditionally this genus belongs to soft-walled monothalamous foraminifera, and Pawlowski *et al.* (2003a) proposed a Precambrian origin for this group. In the molecular phylogeny of foraminifera (Pawlowski *et al.*, 2002a, 2013) the genus *Psammophaga* is included in clade E of the monothalamids. The extraordinary

molecular diversity of monothalamous foraminifera has been documented by Majewski *et al.* (2007), Habura (2008) and Gooday *et al.* (2011). Several *Psammophaga* species have recently been described based on molecular and morphological characters (Pawlowski & Majewski, 2011; Ballero *et al.*, 2013). One of these species, *Psammophaga magnetica*, found in shallow-water Antarctic sediments, selectively ingests magnetite, titaniferous magnetite, and other detrital minerals such as feldspar and quartz grains, concentrating them close to the aperture (Pawlowski & Majewski, 2011). Another species, *Psammophaga sapela*, collected from salt marshes and mudflats along the coast of Georgia, U.S.A., ingests and stores different mineral phases, including ilmenite and zircon (Ballero *et al.*, 2013). Both papers suggest that these two species are able to select and accumulate heavy minerals as ballast, although neither study quantified these minerals in the cytoplasm of *Psammophaga* and compared them to the mineral composition of the sediments where they were found.

Faunal studies of living benthic foraminifera from the central Adriatic Sea have revealed the seasonal occurrence of individuals of *Psammophaga* sp. (Sabbatini *et al.*, 2012). Fluctuations in their density apparently reflect an opportunistic response to pulses of high-quality organic carbon, suggesting a possible role for the species as a shallow-water benthic eutrophication indicator. However, as stated above, the types of minerals ingested by these foraminifera in the Adriatic Sea have not been investigated previously.

The mineral composition of central Adriatic Sea sediments reflects the composition of the drainage basins of the adjacent rivers. The Po River is the most important, and its drainage basin includes the western and central Alps and the Ligurian-Emilian portion of the northern Apennines. As a consequence, the main mineral phases found in the central Adriatic sediments are calcite, dolomite, quartz, clay minerals (muscovite-illite, chlorites, and smectite), and feldspars, with occasional occurrences of amphiboles and serpentine (Dinelli & Lucchini, 1999). Heavy minerals like ilmenite, rutile, and zircon are generally present, but in very low abundance (Pigorini, 1968; Brondi *et al.*, 1979).

The above cited literature, reporting on mineral ingestion by individuals in different environmental settings, stimulated us to investigate the contents of *Psammophaga* from the Adriatic Sea in order to explore the mineralogical phase selection and possible cellular mechanisms underlying this phenomenon.

MATERIALS AND METHODS

Analyses of the ingested minerals in *Psammophaga*

Microscopic analyses, mineralogy, and petrography

Replicated samples ($n = 5$) for this study were collected from five transects, each with three stations, perpendicular

to the coast in the central Adriatic Sea in 12–17 m water depth using a Van Veen grab (Figs 1 and 2 and S1). The specimens were isolated from the upper 2–3 cm of surface sediments of three replicates of each station. Immediately after recovery, the sediment samples were gently washed, and living *Psammophaga* individuals were picked from the >90 μm residues; 23 selected specimens were prepared for Scanning Electron Microscopy (SEM).

The remaining sediment residues were fixed in 10% formalin buffered with sodium borate, with 2 mL of Rose Bengal solution (1 g L^{-1}) for population studies of living stained foraminiferal assemblages. A total of 291 *Psammophaga* specimens were picked.

Living specimens were photographed after isolation using a Nikon Eclipse E 600 POL stereomicroscope with transmitted light. Scanning Electron Microscope micrographs were obtained using a ZEISS SUPRA 55 VP SEM with a 3rd generation GEMINI field emission column, allowing a spatial image resolution down to 1.0 nm, in scattered (SE) and backscattered (BSE) modes, at the University of Paris VI-UMPC.

Chemical compositions of mineral grains inside 17 *Psammophaga* specimens were analysed using an energy dispersive X-ray (EDS) microanalysis system (SAHARA Silicon Drift Detector with PGT's Spirit Software, Rocky Hill, NY, USA) allowing high counting rates, and related cartographies were produced. Hyperspectral X-ray images were produced using the SAHARA Silicon Drift Detector with the same analytical conditions (15 kV accelerating voltage, 7 mm working distance, and a beam current of 8 nA).

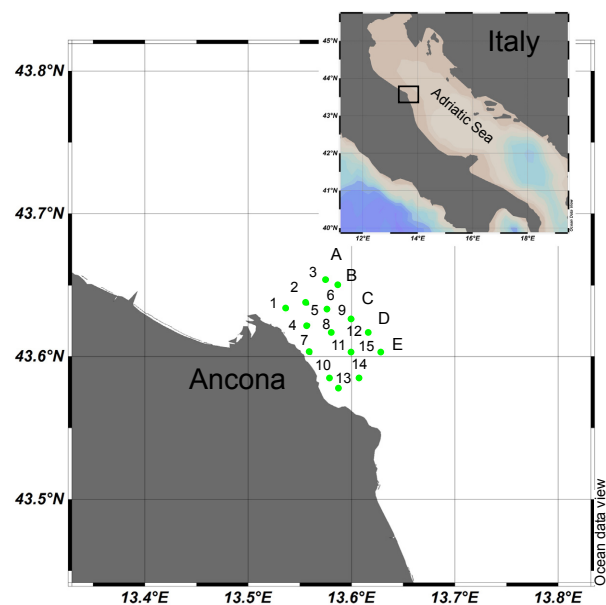


Fig. 1 Location map.

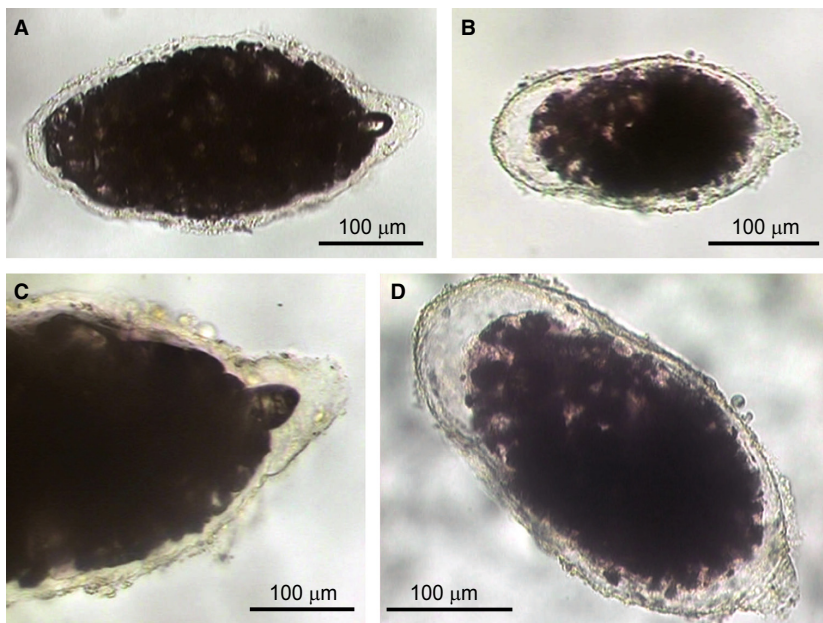


Fig. 2 Type specimens for *Psammophaga zirconia* sp. nov. preserved in 10% formalin from the Central Adriatic Sea. (A–D) Holotype and paratype from station D11 (Portonovo, Central Adriatic Sea). In (A) holotype specimen (DISVA UPM 2015-1) of 375 µm length; in (B) paratype specimen (DISVA UPM 2015-2) of 275 µm length. In (C) and (D) details of the terminal aperture, single and flexible at the end of a very short neck. The wall, thin and transparent with a shiny surface, is also visible. (A) Light microscope photograph of holotype DISVA UPM 2015-1, 375 µm length. (B) Light microscope photograph of paratype DISVA UPM 2015-2, 275 µm length. (C) Light microscope photograph of holotype DISVA UPM 2015-1. (D) Light microscope photograph of paratype DISVA UPM 2015-2.

The size, shape, and chemical composition of the crystals found inside 4 *Psammophaga* individuals were determined using a Philips XL30 SEM with SE and BSE detectors for imaging and EDS for analysis at Dipartimento di Scienze della Terra, Università di Pisa. The individuals were broken and smeared onto a glass slide and carbon coated. A total 115 crystals inside *Psammophaga* were imaged by SEM–SE and BSE detectors, collecting size/shape data for every crystal analysed by SEM–EDS. Furthermore, a volume evaluation of the heavy mineral grains inside four *Psammophaga* cytoplasm was performed using the measured dimensions of the crystals (see Table S1).

Magnetic analyses

The magnetic properties of *Psammophaga* individuals were investigated using a Princeton Measurements Corporation MicroMag 2900 alternating gradient magnetometer (AGM) at the Istituto Nazionale di Geofisica e Vulcanologia (INGV) in Rome. We chose to use an AGM (rather than a vibrating sample magnetometer) to maximize sensitivity and avoid potential inaccuracies caused by movement of *Psammophaga* individuals during sample vibration.

We measured remanent magnetization during stepwise acquisition of an isothermal remanent magnetization (IRM) up to 1 tesla (T); the remanent coercive force (B_{cr}), evaluated by stepwise back-field application on the saturation IRM; hysteresis loops; and first-order reversal curves (FORCs). We performed FORC analyses (Roberts *et al.*, 2014) to characterize magnetostatic interactions and magnetic domain state distributions in the studied samples. Analyses were made with a field increment of 2 mT, H_u ranging from –60 to +60 mT, H_c from 0 to 120 mT, an averaging time of 100 ms, and $N = 137$

measured FORCs. Data were processed, smoothed, and plotted using the FORCINEL program (Harrison & Feinberg, 2008). A smoothing factor of 5 was applied to data. Finally, we evaluated the possible contribution of superparamagnetic grains (SP grains) to the total remanence using the method of Wang *et al.* (2010), which works by monitoring the viscous decay of an applied IRM. Assuming that the room-temperature viscous decay of the IRM 100 s after its application is due to thermal relaxation of the magnetization carried by the SP fraction, the SP particle percentage can be estimated as $M_{RS}(SP)\% = 100 (M_{RS0} - M_{RS100})/M_{RS0}$, where M_{RS0} is the remanence measured immediately after application of a 1 T saturating field and M_{RS100} is the remanence measured 100 s after field application.

Sediment analyses: sedimentology, petrography, and geochemistry

The collected samples were used for grain-size analysis of surface sediments. The sample locations are given in Fig. 1. Grain-size analyses were carried out on wet sediment samples pre-treated with H_2O_2 -16 vol. solution to remove organic matter. The coarser fractions (>63 µm) of samples were analysed by sieving using the sifting machine FRITSCH analysette 3 (Spartan pulverisette 0) while the finer fractions (<63 µm) were analysed by X-ray sedigraph (Micrometrics 5100). Before sieving, the samples were dried to determine their dry bulk masses, and 25 g of the dry sediment was removed for bulk sediment measurements. Sieving was performed with a vibration amplitude of 1.5 mm and the sieving time was 20 min in total. Eight grain-size fractions from >500 to >63 µm (See Table S2)

were obtained using eight stacked sieves. Grain size distribution from 63 to 0.6 μm was determined following the method described in Spagnoli *et al.* (2014).

SEM and EDS investigations, as described in the paragraph 2.1.1, were also performed on the bulk, the coarser (>63 μm), and the finer fraction (<63 μm) of the sediment samples from the same stations used for foraminiferal analyses (Transect D, A3 and E15 sites in Fig. 1), in order to assess the distribution and the quantity of the minerals in the sediment. For this study, sediments were set in a resin epoxy (Araldite 2020, XW 396/XW 397) at room temperature, and then highly polished (by alumina powder 0.5 μm on a 'Escil ALD' polishing cloth). Finally, with the aim of comparing the mineral distribution between *Psammophaga* and the host sediment, three sediment samples were collected at the sites A3, D12 and E15. About 1 g of the <63 μm fraction, after ultrasonic cleaning, was placed in liquid Na-polytungstate (density = 2.95 g cm⁻³). The suspension was centrifuged at 1000 $\times g$, and 900 crystals of the sunken fraction were investigated for size, shape and composition by SEM-EDS (see Table S1). Minerals were identified based on cationic proportions and, for euhedral crystals, also on crystal morphologies and faces, leading to unequivocal identification of zircon and ilmenite; as for the Ti oxide, the prismatic and fibrous shapes can be ascribed to rutile, and the di-pyramidal crystal are likely anatase.

Major (SiO₂, Al₂O₃, TiO₂, Fe₂O₃, MnO, CaO, MgO, K₂O, Na₂O, P₂O₅) and trace (V, Cr, Co, Ni, Cu, Zn, Ga, As, Rb, Sr, Y, Zr, Nb, Ba, La, Ce) element analyses were performed on the bulk and the finest fraction (<63 μm) of the sediment samples from the same stations used for foraminiferal analyses, by means of X-ray Fluorescence spectrometry using a Panalytical Axios4000 spectrometer on pressed powder pellets following the methods of Franzini *et al.* (1972, 1975), Leoni & Saitta (1976), and Leoni *et al.* (1986). Accuracy was tested by analysing international reference standards: differences with reference values were lower than 5%, except for trace elements with concentrations lower than 10 $\mu\text{g g}^{-1}$ (10% relative difference). The Loss on Ignition was determined gravimetrically after overnight heating at 950 °C.

Molecular study

DNA extraction, PCR amplification, sequencing

DNA extractions were performed on three single specimens using guanidine lysis buffer. The primer pairs s14F3-s20 and 14F1-s20 were used to amplify and re-amplify the 3' end fragment of SSU rDNA (Pawlowski, 2000). The amplified PCR products were purified using High pure PCR Purification Kit (Roche Diagnostics, Risch-Rotkreuz, Switzerland), cloned with the TOPO TA Cloning Kit (Invitrogen, Carlsbad, CA, USA) following the manufacturer's instructions, and transformed into competent

Escherichia coli. Sequencing reactions were performed using the BigDye Terminator v3.1 Cycle Sequencing Kit (Applied Biosystems, Foster City, CA, USA) and analysed on a 3130XL Genetic Analyzer (Applied Biosystems).

Phylogenetic analysis

Eight partial sequences of *Psammophaga zirconia* SSU rDNA were obtained and added to an existing database using the Muscle automatic alignment option as implemented in Seaview vs. 4.3.3. (Gouy *et al.*, 2010). 54 sequences of the genus *Psammophaga* and three sequences of the genus *Vellaria* were aligned. The alignment contains 1033 sites, of which 391 were used for analysis. Based on MEGA5 (Tamura *et al.*, 2011), a GTR model of evolutionary changes was selected for all analyses. Phylogenetic trees were constructed using maximum likelihood (ML) method using RaxML as implemented in BlackBox (Stamatakis *et al.*, 2008).

SYSTEMATICS

We follow Adl *et al.* (2005) in placing the Foraminifera in the supergroup Rhizaria. Traditionally, the monothalamous foraminifera were split between agglutinated and organic-walled genera, placed in the orders Astrorhizida and Allogromiida respectively (Loeblich & Tappan, 1987). This taxonomic division was however invalidated by molecular phylogenies, showing agglutinated and organic-walled monothalamous species intermingling in ribosomal trees (Pawlowski *et al.*, 2002a,b, 2003a,b, 2005). Here, we refer to the genus *Psammophaga* assigned by Pawlowski & Majewski (2011) and Pawlowski *et al.* (2013), and propose to describe a new species of *Psammophaga* based on the traditional description of morphological features.

Supergroup RHIZARIA Cavalier-Smith, 2002

Phylum FORAMINIFERA d'Orbigny, 1826

Class 'Monothalamea' Pawlowski *et al.*, 2013;

Clade E (Pawlowski *et al.*, 2002a)

Genus *Psammophaga* Arnold, 1982

Psammophaga zirconia Sabbatini, Bartolini, Morigi, sp. nov.

Etymology

The species name *zirconia* refers to the nature of the mineral inclusions, namely zircon that this taxon selectively ingests.

Type material

Type specimens, collected at station D11 (Portonovo) in the Adriatic Sea (43.60335°N, 13.61175°E, 14.5 mwd) and preserved in 10% formalin buffered with sodium borate, were deposited at the Department of Environmental and Life Science (Di.S.V.A.), Polytechnic University of

Marche, Ancona (Italy) under the following registration numbers: holotype DISVA UPM 2015-1 (Fig. 2A,C); paratypes: DISVA UPM 2015-2 (Fig. 2B,D) and DISVA UPM 2015-3a-c (Fig. S1A,D,G).

A total of 291 specimens, fixed in 10% formalin buffered with sodium borate, with 2 mL of Rose Bengal solution (1 g L^{-1}) were analysed for the morphological and population studies.

Diagnosis

Test free, single-chambered, pyriform, elongate, or spherical in shape with a single simple terminal aperture; the wall thin and transparent, appears to be mainly organic with a sparse surface dusting of fine particles. The cell body does not entirely fill test lumen; abundant mineral inclusion retained throughout the entire cytoplasm.

Description

Pyriform, elongate or spherical theca with length usually ranging $\sim 0.20\text{--}0.70 \text{ mm}$. The apertural (proximal) end is usually rounded and tapering at the distal end toward a large, simple aperture (Figs 2 and 3C). The wall is thin and transparent with a shiny surface. The aperture is clearly visible, single and flexible which may occur at the end of a very short neck; it seems not to be prolonged into any internal structure (Fig. 2C). The aperture is presumed to be sufficiently plastic to allow for the passage of sediment grains of various sizes. Where visible the cytoplasm is white and fine grained and often drawn out into a point immediately inside the aperture. The cytoplasm contains numerous

cytoplasmic inclusions of mineral grains that typically appear to fill the entire test (Figs 2 and 3C). Pseudopodia reticulate solely from a short peduncle that emerges from the aperture through which food and sediment grains also pass. While sorting both living and Rose Bengal stained specimens, strong brightness of *Psammophaga* specimens was noted together with magnetism of some analysed individuals. As is typical of the genus, *P. zirconia* ingests and retains abundant mineral inclusions and appears to prefer heavier minerals, in particular zircon and rutile.

Molecular features

Eight partial SSU rDNA sequences were obtained from 3 *P. zirconia* specimens collected at the type locality (Fig. 4). The sequences were submitted to GenBank (Accession numbers LN886765 to LN886772). Sequence length ranges from 877 to 1024 nt, the GC content ranges from 46.2% to 46.8%. Phylogenetic analysis of the eight sequences groups them into a strongly supported clade (96% BV).

Distribution

Living *P. zirconia* was found at 15 sites from the central Adriatic Sea, between 12 and 17 mwd (Fig. 1). It was commonly found in low numbers, <0.5 specimens per 10 cm^{-2} , but at one location (D11) at 14.5 mwd it occurred in great abundance (>150 specimens per 10 cm^{-2}) following seasonal input of organic matter. Faunal studies of living benthic foraminifera from the central Adriatic Sea have described the occurrence, seasonally

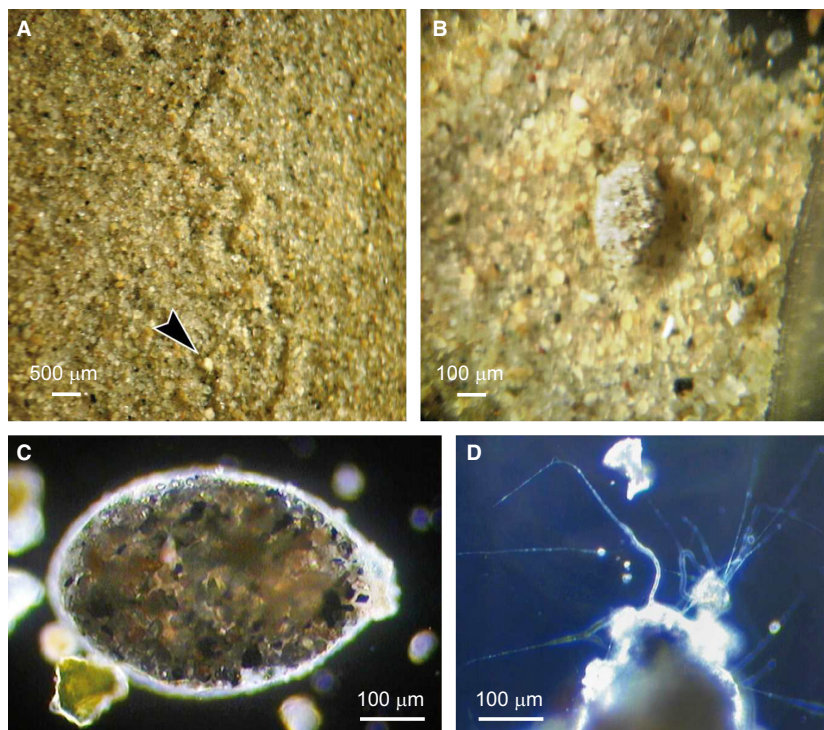


Fig. 3 Stereomicroscope photographs of living *Psammophaga zirconia* individuals. (A) Track of the *P. zirconia* movement in the sediment; arrow indicates the final position of the specimen. (B) The appearance of *P. zirconia* in the sediment where it lives. (C) Living *P. zirconia*; intracellular mineral inclusions are visible. (D) Pseudopodial activity of *P. zirconia*.

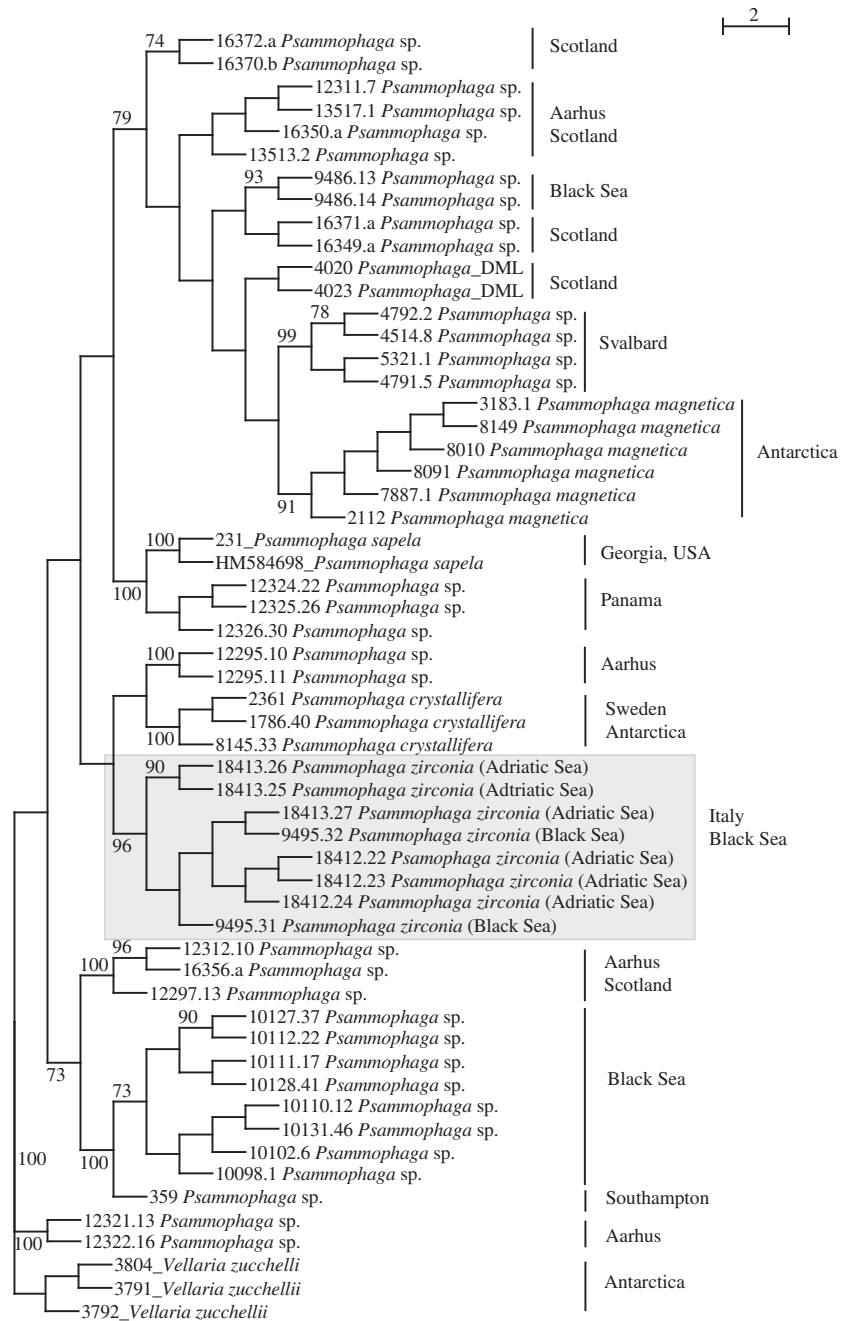


Fig. 4 Maximum likelihood phylogenetic tree of monothalamid foraminifera showing the position of the new species *Psammophaga zirconia* described in this study. Numbers at nodes correspond to bootstrap values higher than 70%.

important, of individuals of the genus *Psammophaga* (Sabbatini *et al.*, 2012); their density is associated with the quantity of available organic matter on the sea floor, and the specimens show opportunistic behavior in response to the pulses of high-quality organic carbon, suggesting a possible role for the species as shallow-water benthic eutrophication indicator.

Remarks

Psammophaga zirconia differs from other described species of *Psammophaga* including *P. crystallifera* (Dahlgren,

1962), *P. simplora* Arnold, 1982; *P. magnetica* Pawlowski & Majewski, 2011 and *P. sapela* Ballero *et al.*, 2013. Morphologically, *P. zirconia* most closely resembles *P. simplora* and *P. sapela*, which populations include pyriform, spherical and elongate individuals; *P. crystallifera* and *P. magnetica* have both a more elongated test; conversely *P. zirconia* has an organic wall composition like *P. magnetica*, a feature that it does not share with other *Psammophaga* species. The new species has a peduncle as in other *Psammophaga* species except for *P. simplora* lacking this morphological characteristic. *Psammophaga* species have

predominantly mineral inclusions concentrated around the apertural end and they seem to be more widely spread in *P. sapela* and *P. crystallifera*. In all observed individuals of the new species, cytoplasmic mineral grains appear to fill the test entirely (Figs 2, 3 and 5 and S2). Although *P. zirconia* shares some morphological peculiarities with all *Psammophaga* species, it differs in mineral inclusion features. The new species incorporates heavy minerals and predominantly selects equidimensional zircon, while *P. magnetica* ingests magnetite along with minor amounts of other lighter minerals; in other *Psammophaga* species, authors described a mixture of mineral grains, most of them heavy. As for *P. zirconia*, the presence of zircon, ilmenite and Ti oxides was also reported in *P. sapela*, although their quantitative proportion in the cytoplasm remains undescribed. If left isolated in a culture dish with no movement or extraneous sediment overnight, *P. zirconia* does not egest most of its mineral inclusion as observed in *P. sapela* (Ballero *et al.*, 2013). *P. zirconia* inhabits geographically and ecologically distinct settings with respect to *P. magnetica*, dominant in polar habitats, and *P. sapela*, in marsh and mudflat areas.

Phylogenetically, *P. zirconia* branches at the base of a clade containing *P. crystallifera* and *Psammophaga* sp. from Denmark, but the branching is not supported (Fig. 4). The six sequences obtained from the Adriatic samples are very similar to two unpublished sequences from the Black Sea, collected near Sevastopol (Gooday *et al.*, 2011). Together all these sequences form a strongly supported (96% BV) clade, which is considered here as corresponding to the new species. It has to be highlighted that the genetic diversity of the genus *Psammophaga* is very high. Our phylogenetic analyses group all *Psammophaga* sequences into

17 clades, each of which probably corresponds to a separate species. However, none of these clades, including all described species, is closely related to *P. zirconia*, reinforcing the arguments for describing it as a new species.

RESULTS

The SEM and EDS analyses performed on the cytoplasm of *P. zirconia* specimens allowed us to identify the presence of different minerals and also the shape and composition (and hence the nature) of the mineral crystals. These analyses revealed that all analysed specimens are filled with heavy minerals among which zircon particles are largely dominant. The total volume of crystals throughout the *Psammophaga* cytoplasm reaches more than 70%, as also supported by SEM photographs and related EDS cartographies (Figs 5 and S2). Quantitative examination performed on four previously broken *Psammophaga* individuals by SEM and EDS showed that the mineral grains comprised 51% nearly equidimensional zircons, 27% Ti oxides (mainly rutile), 11% ilmenite, and 3% magnetite, along with minor amounts of other lighter minerals (Fig. 6). Aggregates ($10 \times 20 \mu\text{m}$) of μm -sized halite cubes have been observed, which are possibly linked to precipitation from individuals stained with Rose Bengal solution. Once the numbers of crystals are converted to volumes, more than 80% is represented by zircon, with only a mere 20% by other heavy mineral grains (Ti oxides, ilmenite, and magnetite; Fig. 5; see Table S1 and Fig. S2). The magnetic analyses, performed on cells of *P. zirconia*, consistently indicated the presence of magnetite (Fig. S3). More than 90% of saturation magnetization was reached in a field of 200 mT and the coercivity of remanence is in the range of

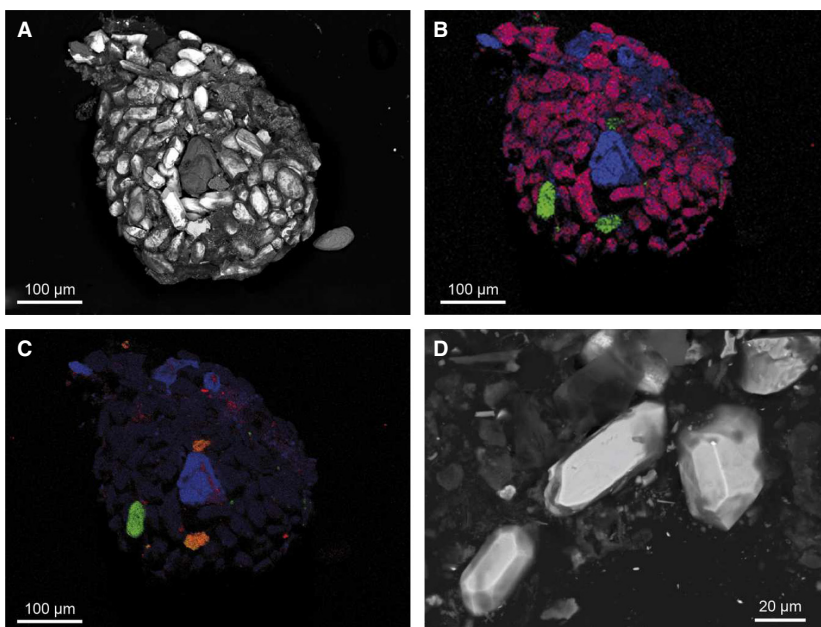


Fig. 5 SEM photographs and related EDS cartographies of living *Psammophaga zirconia* specimen. (A) SEM BSE photograph of *P. zirconia* filled with mineral grains. (B) Combined color image of three elements (Red = Zr, Green = Ti, Blue = Si) from an elemental analysis of the same specimen in (A). Minerals in pink are zircons, in green Ti oxides, in blue silicates and quartz. (C) Results of differential elemental analysis mapping (Red = Fe, Green = Ti, Blue = Si). Identified minerals in red are Fe oxides, in orange ilmenite, in green rutile, in blue silicates and quartz. (D) Zircon crystals inside the cell of *P. zirconia*; different specimen from (A–C). Images resolution: 1024 × 768 × 16 bits.

15 mT. The FORC diagram has a peak near the origin with open contours that diverge toward the H_u axis; this is consistent with the presence of low-coercivity (fine) multidomain magnetite grains (MD grains) (2–10 μm) which, in turn, is consistent with the size of the intracellular Fe oxides revealed from elemental analysis by EDS (Fig. S2). However, the absence of a viscous decay of magnetization (Wang *et al.*, 2010) seems to exclude the concomitant presence of ultrafine magnetite fractions (cubic SP, 20–30 nm).

On the basis of these results we further explored the grain size distribution and chemical composition of the sediments in the sites where individuals were collected, in order to understand possible relationships between *P. zirconia* density and sediment characteristics.

Our results show that the grain-size distribution in surface samples is mostly clayey silt and silt (Shepard, 1954). Coarser sediments (sand >30%) are dominant near-shore at

shallow depths and at the southernmost stations. Sites located further away from the coast have a more abundant silt fraction, while northernmost stations are richer in clay (Table S2).

Geochemical analyses results indicate that silicate and quartz are the dominant minerals in all samples ranging from 31.93 (%) to 42.88 (%) in the bulk sediment and 34.11 (%) to 43.39 (%) in the finer fraction (<63 μm) (Table S3). Zr concentrations range from 56 to 194 $\mu\text{g g}^{-1}$ (10–183 ppm) and its value is higher (50–328 $\mu\text{g g}^{-1}$; 126–329 ppm) in the finer fraction (<63 μm) of the studied samples with increasing values to the south of the studied transects (Fig. 1). The results for Ti (1320–3540 $\mu\text{g g}^{-1}$) and Fe (15 180–36 440 $\mu\text{g g}^{-1}$) display a mainly increasing trend with distance from the coastline (Table S3).

Additionally SEM and EDS investigations performed on bulk sediment samples, on the separate coarsest (>63 μm) and finest (<63 μm) fractions, reveal that silicates and quartz dominate (Fig. S4B,C), while zircon, ilmenite, Fe and Ti oxides are rare minerals. In detail, in the analysed finest fraction of the sites A3, D12 and E15, 1% of minerals are zircon, 4% ilmenite, 4% Ti oxides (mainly rutile) and 3% Fe oxides (magnetite) (Fig. 6).

DISCUSSION

Our data point to an unusually high concentration of zircon minerals in the *P. zirconia* cytoplasm, which contrasts with the extreme rarity of Zr in the sediment, strongly suggesting a selectivity of mineral ingestion in these organisms (Figs 6 and S4).

To a lesser extent, but more significantly, Ti–Fe-bearing minerals such as ilmenite, Ti oxides, and magnetite are also accumulated along with the zircon crystals; they all are rare minerals in the sediment and constitute the densest mineral component within a sediment in which silicates and quartz crystals dominate (Figs 6 and S4). The Zr is associated only with zircon and no other mineralogical phases, suggesting a very low abundance of this mineral in the sediment. In the case of Ti, however, the mineralogical phases are various: Ti is associated with rutile, ilmenite, and titanite and Fe with magnetite, ilmenite, and pyrite. Moreover, our mineralogical distributions of sediment are consistent with data published by Spagnoli *et al.* (2014) for the Central Adriatic Sea, reporting low concentrations of Zr, Ti, and Fe oxides, and a dominance of silicates and quartz.

Significantly, zircon and Ti oxides are both selectively concentrated in the cell (respectively 51% and 27%, vs. 1% and 4%), whereas Fe oxides (magnetite) and ilmenite show cytoplasmic concentrations comparable to those found in the sediment (Fig. 6). Here we address the question of how foraminifera can select minerals, in order to understand the possible advantages that this behavior confers in a morphologically simple organism such as *P. zirconia*.

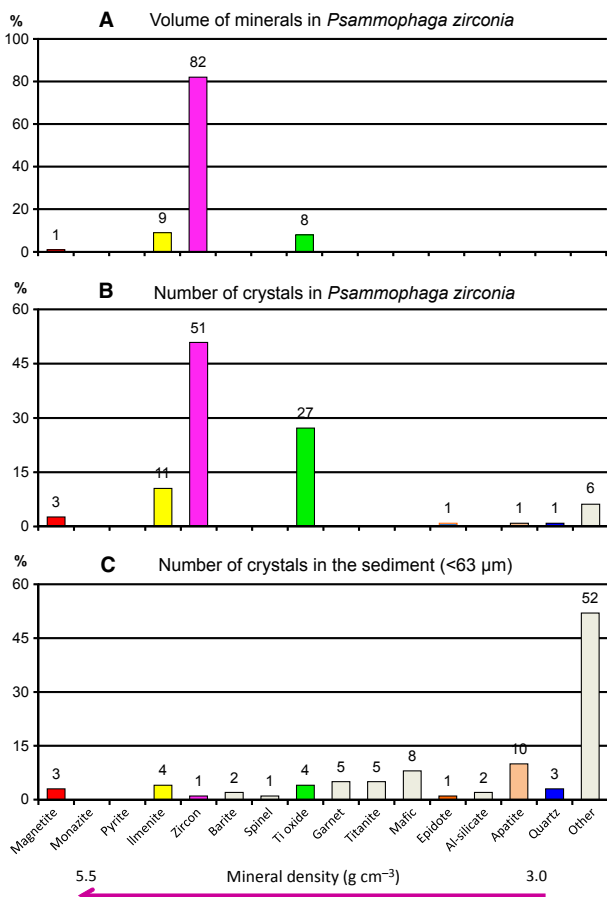


Fig. 6 (A) Percentage of volume that heavy minerals occupy in the 4 *Psammophaga zirconia* cells. (B) Percentage of minerals calculated on the basis of counted crystals inside 4 *P. zirconia* specimens. (C) Percentage distribution of the 16 minerals in three sediment samples of the <63 μm fraction in the 900-point analyses. Size and nature of the mineral crystals are determined by SEM–EDS. Arrow indicates the mineral density increase.

Mechanism of mineral grain incorporation

In the absence of any specific literature dealing with the ingestion or retention of mineral grains, we discuss the most recent developments in the field of foraminifera, with particular regard to monothalamid foraminifera. Agglutinated fossilized foraminifera exhibit two modes of grain selectivity in their test construction. Makled & Langer (2010) review references on mineral selection according to (i) size and (ii) selectivity of specific minerals or particles. Reports of grain-size selection appear to be more common (Lipps, 1973; Bowser & Bernhard, 1993) than selection on the basis of particle composition. In the latter case, the selection of mineral particles by foraminifera involves interactions between the molecules present in the reticulopodia and on the surface of the mineral (Makled & Langer, 2010). The ability to form electrostatic or hydrogen bonds with the mineral surfaces relies upon the glycoprotein-rich surfaces of reticulopodia (Pawlowski & Majewski, 2011). This led Makled & Langer (2010) to speculate that minerals of high electron density form charged dipoles that are particularly easy for foraminiferal pseudopods to detect. Furthermore, since organic compounds, such as catechol of the type found in other marine adhesives (Sever *et al.*, 2004), are known to favor adsorption onto TiO₂ surfaces (Vasudevan & Stone, 1996), we suggest that catechol or a similar functional group is present in the reticulopodia membrane of *Psammophaga*, and that this affinity provides a mechanism for mineral selection (Cole & Valentine, 2006). In addition to this possible electrostatic interaction, the isoelectric point (IEP) could also refine the chemical recognition, by mimicking the flotation process mediated by the organic components (Hoşten, 2001). Thus, we infer that the functional groups of the pseudopod membrane glycocalyx could act as flotation agents to separate and isolate particular minerals from the sediment in which *Psammophaga* species live. We suggest that the selection and concentration of minerals for monothalamous soft-walled and agglutinated foraminifera (whether ingested or incorporated in the test) is based on the same chemical mechanism as we hypothesize for *Psammophaga* individuals. Such a mechanism depends on the IEP of the mineral and the metabolically regulated pH of the cell. In the presence of high values of cellular pH, minerals such as silicates and metallic oxides with IEP values between neutral and basic seem to interact preferentially with the organic component of the pseudopodia (Liu *et al.*, 2000). This mechanism could explain the selection of minerals such as zircon and Ti oxides (IEP values ranging from 5.5 to 5.9 for zircon and 5.7 to 6.1 for Ti oxides respectively), which, due to a basic cellular pH (up to 10) above the IEP of the minerals themselves, would be easily recognizable when in contact with the filaments of the glycocalyx exposed on the pseudopodial membrane.

Advantage of selective mineral inclusions

The reason for concentrating heavy minerals in foraminiferal tests has been discussed in several papers. The first is Heron-Allen (1915) who speculated that the concentration of heavy minerals as a result of rapid settlement following wave/current agitation could increase the chances of foraminifera agglutinating these denser particles. A selective behavior was then described in different taxonomic groups of agglutinated foraminifera, namely *Bathysiphon*, *Nothia*, *Psammospaera*, *Psammosiphonella*, *Ammobaculites*, *Reophax*, *Recurvoides*, *Textularia*, *Trochamminoides* and *Paratrochamminoides* (Kaminski *et al.*, 2008; Makled & Langer, 2010; Waskowska, 2014), which build their tests using specific mineral grains secured in various kinds of cements referred to as tectin, consisting of protein and complex carbohydrate (Lipps, 1973; Gooday & Claugher, 1989).

In contrast, the ingestion of heavy minerals by soft-walled, single-chambered taxa such as *Psammophaga* has rarely been discussed; Nyholm (1957) and Dahlgren (1962) proposed that the presence of mineral grains inside their cells helps light, soft-walled foraminifera to anchor themselves in very soft mud. Therefore the ingestion of heavy minerals by *Psammophaga* may be related to problems with buoyancy. Also, a group of large agglutinated foraminifera, namely Xenophyophores, show a similar ballasting behavior when ingesting barite crystals (Gooday & Nott, 1982; Hopwood *et al.*, 1997), or other minerals, tentatively identified as ilmenite, rutile, and anatase (Rothe *et al.*, 2011). It is possible that, in addition to the ballasting effect, the foraminifera ingest zircon instead of dark minerals of similar specific density for camouflage in the silicate-dominated sediment, allowing them to escape predators.

In addition, we can speculate that the location of mineral grains in different parts of the cell may reflect different strategies for detecting the best food sources (bacteria or organic matter with a high lipid content). For instance, in *P. magnetica*, the minerals are concentrated at the anterior end of the cell (see Fig. 2A–C in Pawlowski & Majewski, 2011), which may serve to bring the aperture into contact with the sediment and potential food sources. In *P. sapela*, ingested sediment grains are dispersed throughout and concentrated toward the center of the cell body during gametogenesis (see Fig. 7 in Ballero *et al.*, 2013). Ballero *et al.* (2013) found bacterial colonies within the organic bioadhesive of *P. sapela* that specimens use to cement clay platelets of its agglutinated theca. Since bacteria constitute a large part of the food of many foraminifera (Lee, 1980; Langezaal *et al.*, 2005), these authors suggest that sediment uptake in the form of mineral grain ingestion allows microbiota to adhere to sediment particles. However, the more uniform distribution of minerals in *P. zirconia* sug-

gests a different dietary strategy, as the aperture is not necessarily oriented into the sediment, as observed in culture experiments.

As stated above, most of our knowledge of foraminiferal behavior in selecting heavy minerals is related to ingestion mechanisms. Nevertheless, we cannot exclude the possibility that heavy mineral grains can selectively be retained in the cytoplasm from the rough sediment randomly ingested by the organism. Currently, there is no foraminiferal literature focusing on this topic and therefore we cannot discriminate between differential ingestion and differential retention; it is however noteworthy that in both cases organisms show a selection behavior whose advantages were previously described.

Geological implications

A deeper understanding of the sediment uptake dynamics in *P. zirconia* and other *Psammophaga* spp. is essential, also to understand the evolution of early foraminifera and their relationship with modern single-chambered taxa contextualizing our results in the geobiology field. As suggested by molecular clock estimation, the radiation of monothalamous foraminifera probably occurred between 1150 and 690 Ma, largely predating the Cambrian origin of multi-chambered species (Pawłowski *et al.*, 2003a). In the fossil record, the earliest foraminifera (single- and multi-chambered agglutinated taxa) are described from early Cambrian sediments (Culver, 1991, 1994), while putative foraminifera are reported in Neoproterozoic fossil faunas (Lipps & Rozanov, 1996; Gaucher & Sprechmann, 1999; McLroy *et al.*, 2001; Bosak *et al.*, 2011a, 2012). Probably some of these early foraminifera (including *Psammophaga*) may have had mineral-rich tests (Pawłowski *et al.*, 2003a) and could have thrived in microbially dominated, oxygen-poor environments (Bernhard *et al.*, 2006), leaving a fossil record. However, the difficulty of recognizing unambiguously ancestral monothalamous foraminifera in the fossil record might be related to a combination of factors, such as preservation in the sediments, adverse paleoenvironmental conditions and the absence of clear morphological characters distinguishing them from other morphologically simple testate amoeboid eukaryotes (Bosak *et al.*, 2011a, 2012).

As matter of fact, Bosak *et al.* (2011a) described forms with an oval flexible wall made of organic and finely agglutinated particles in post-Sturtian (716–635 Ma) cap carbonates, and interpreted them as possibly lobose testate amoebae (Amoebozoa) with the capacity for an active, biological agglutination of detrital minerals. However, authors do not exclude the possibility that some of these fossil structures might also be related to early foraminifera, in particular some modern monothalamous agglutinated foraminifera (Bosak *et al.*, 2011a, 2012). Specimens reported

in Fig. 3 of Bosak *et al.* (2011a) are indeed morphologically very similar to saccamminid taxa, including representatives of the genus *Psammophaga*. In this context, *Psammophaga* species are modern representatives of mineral-rich test organisms, and they are saccamminid with a flexible wall. As all *Psammophaga* species sharing the presence of large mineral crystals branch within a single clade E, it is very likely that also the behavior of ingesting and storing the mineral particles has very ancient origins. In fact, *Psammophaga* can be viewed as a packaging agent for fine-grained, reactive (magnetite), heavy mineral phases, encapsulating them in an organic matrix.

Furthermore, the emerging record of protist microfossils (Bosak *et al.*, 2011a,b, 2012) and other putative eukaryotes (Maloof *et al.*, 2010) suggests that a fossil *Psammophaga* could be preserved (with or without mineral inclusions); the fact that these authors found eukaryotic body fossils that can be similar to a saccamminid representative supports our inference.

In that case, our observations can contribute to improving knowledge of the ecological behavior and environment of these ‘oval monothalamous microfossils’ of the ancient world. In particular, understanding more about mineralogical phase selection and possible cellular mechanisms behind this behavior might allow them to be used as better indicators of ancient environments (Pike & Kemp, 1996; Schieber, 2009, 2012). Finally, the behavior of some *Psammophaga* species, such as *P. zirconia*, preferentially accumulating a specific mineral in the cell, could favor their fossilization, and the presence of heavy minerals inside could be an additional diagnostic characteristic, preserved through time and helping to describe and identify the fossil monothalamous foraminifera.

CONCLUDING REMARKS

Our results provide the first quantitative observation of the preferential uptake of heavy minerals other than magnetite and Ti oxides by individuals of *P. zirconia*. In particular *P. zirconia* selectively accumulates zircon. Our finding may not be applicable to all *Psammophaga* species because the behavior might be species-specific, but we present solid evidence that the mineral inclusions are not dependent on the compositional features of the sediment where the foraminifera live.

We suggest some behavioral mechanisms allowing the selection and accumulation of the appropriate types of minerals within the cell of *P. zirconia*, which we speculate could be based on the electrostatic interactions between cellular compounds of the foraminiferal reticulopodia (or organic cement) and the mineral surfaces. The most plausible hypothesis regarding the reason for the genus *Psammophaga* to select and ingest zircon and other heavy minerals is that this behavior represents an advantage for remaining stable in

the sediment, and thus a more efficient feeding strategy. Finally, the presence of eukaryotic soft-walled monothalamous microfossils, capable of building a fine aluminosilicate case, in the Precambrian geological record, makes them useful as a valuable record of the early evolution of foraminifera, suggesting that biological agglutination was already present in this group. *P. zirconia* is a new documented example among foraminifera capable of highly intriguing preferential mineral uptake, showing that this behavior could have emerged very early in their evolution.

ACKNOWLEDGMENTS

The authors gratefully acknowledge Andrew J. Gooday (National Oceanography Centre, Southampton) for constructive discussions and for critical assessment of the manuscript. The authors thank Alexandre Lethiers (University UPMC Paris VI) who helped with graphical construction of Figs 2, 3 and 5 and S1, S2, and S4; Irene Pancotti, who helped with the picking work at the microscope, and Alessandro Ferlazzo Ciano who performed faunal and geochemical analysis. The authors are grateful to the editor, the subject editor, and two anonymous reviewers for their constructive comments and suggestions, which helped us to improve the manuscript. This study was supported by the ATM Biomineralization program of the Muséum National d'Histoire Naturelle of Paris (project granted to A. Bartolini); the Swiss National Science Foundation grants 31003A-140766 and 313003A-159709 and the G. and A. Claraz Donation; by the Fondi di Ateneo Università di Pisa to C.M. and Fondi di Ateneo Università Politecnica delle Marche to A.N.

REFERENCES

- Adl SM, Simpson AG, Farmer MA, Andersen RS, Or Anderson (2005) The new higher-level classification of eukaryotes with emphasis on the taxonomy of protists. *Journal of Eukaryotic Microbiology* **52**, 399–451.
- Arnold ZM (1982) *Psammophaga simplora* n. gen., n. sp., a polygenomic Californian saccamminid. *Journal of Foraminiferal Research* **12**, 72–78.
- Ballero DZA, Habura A, Goldstein ST (2013) *Psammophaga sapela* n. sp., a new monothalamous foraminiferan from coastal Georgia, U.S.A.: fine structure, gametogenesis, and phylogenetic placement. *Journal of Foraminiferal Research* **43**, 113–126.
- Bernhard JM, Habura A, Bowser SS (2006) An endobryont-bearing allogromiid from the Santa Barbara Basin: implications for the early diversification of foraminifera. *Journal of Geophysical Research* **111**, G03002.
- Bosak T, Lahr DJG, Pruss SB, Macdonald FA, Dalton L, Matys ED (2011a) Agglutinated tests in post-Sturtian cap carbonates of Namibia and Mongolia. *Earth and Planetary Science Letters* **308**, 29–40.
- Bosak T, Macdonald FA, Lahr DJG, Matys ED (2011b) Putative Cryogenian ciliates from Mongolia. *Geology* **39**, 1123–1126.
- Bosak T, Lahr DJG, Pruss SB, Macdonald FA, Gooday AJ, Dalton L, Matys E (2012) Possible early foraminiferans in post-Sturtian (716–635 Ma) cap carbonates. *Geology* **40**, 67–70.
- Bowser SS, Bernhard JM (1993) Structure, bioadhesive distribution and elastic properties of the agglutinated test of *Astrammmina rara* (Protozoa: Foraminiferida). *Journal of Eukaryotic Microbiology* **40**, 121–131.
- Brondi A, Ferretti O, Anselmi B, Falchi G (1979) Analisi granulometriche e mineralogiche dei sedimenti fluviali e costieri del territorio italiano. *Bollettino della Società Geologica Italiana* **98**, 296–323.
- Cole KE, Valentine AM (2006) Titanium biominerals: titania needles in the test of the foraminiferan *Bathysiphon argentus*. *Dalton Transactions* **3**, 430–432.
- Culver SJ (1991) Early cambrian foraminifera from west Africa. *Science* **254**, 689–691.
- Culver SJ (1994) Early Cambrian foraminifera from the southwestern Taoudeni Basin, West Africa. *Journal of Foraminiferal Research* **24**, 191–202.
- Dahlgren L (1962) *Allogromia crystallifera* n. sp., a monothalamous foraminifer. *Zoologiska Bidrag från Uppsala* **35**, 451–455.
- Dinelli E, Lucchini F (1999) Sediment supply to the Adriatic Sea basin from the Italian rivers; geochemical features and environmental constraints. *Giornale di Geologia* **61**, 121–132.
- Franzini M, Leoni L, Saitta MA (1972) Simple method to evaluate the matrix effects in X-ray fluorescence analysis. *X-ray Spectrometry* **1**, 151–154.
- Franzini M, Leoni L, Saitta M (1975) Revisione di una metodologia analitica per fluorescenza-X basata sulla correzione completa degli effetti di matrice. *Rendiconti della Società Italiana di Mineralogia e Petrologia* **31**, 365–378.
- Gaucher C, Sprechmann P (1999) Upper Vendian skeletal fauna of the Arroyo del Soldado Group, Uruguay. *Beringeria* **23**, 55–91.
- Gooday AJ, Claugher D (1989) The genus *Bathysiphon* (Protista, Foraminiferida) in the NE Atlantic: SEM observations on the wall structure of seven species. *Journal of the Natural History* **23**, 591–611.
- Gooday AJ, Nott JA (1982) Intracellular barite crystals in two xenophyophores: *Aschemonella ramuliformis* and *Galatheammmina* sp. (Protozoa: Rhizopoda) with comments on the taxonomy of *A. ramuliformis*. *Journal of the Marine Biological Association of the United Kingdom* **62**, 595–605.
- Gooday AJ, Oksana V, Pawlowski J (2011) New genera and species of monothalamous Foraminifera from Balaclava and Kazach'ya Bays (Crimean Peninsula, Black Sea). *Marine Biodiversity* **41**, 481–494.
- Gouy M, Guindon S, Gascuel O (2010) SeaView Version 4: a multiplatform graphical user interface for sequence alignment and phylogenetic tree building. *Molecular Biology and Evolution* **27**, 221–224.
- Habura A (2008) A bush not a tree: the extraordinary diversity of cold-water basal foraminiferans extends to warm-water environments. *Limnology and Oceanography* **53**, 1339–1351.
- Harrison R, Feinberg J (2008) FORCinel: an improved algorithm for calculating first-order reversal curve distributions using locally weighted regression smoothing. *Geochemistry Geophysics Geosystems* **9**, 1–11.
- Heron-Allen E (1915) A short statement upon the theory, and the phenomena of purpose and intelligence exhibited by the protozoa, as illustrated by selection and behaviour in the Foraminifera. *Journal of the Royal Microscopical Society* **6**, 547–557.

- Hopwood JD, Mann S, Gooday AJ (1997) The crystallography and possible origin of barium sulphate in deep sea rhizopodprotists (Xenophyophorea). *Journal of the Marine Biological Association of the United Kingdom* **77**, 969–987.
- Hoşten Ç (2001) Micro-floatability of rutile and zircon with soap and amine type collectors. *Physico Chemical Problems of Mineral Processing* **35**, 161–170.
- Kaminski MA, Armitage DA, Jones AP, Coccioni R (2008) Shocked diamonds in agglutinated foraminifera from the Cretaceous/Paleogene Boundary, Italy – a preliminary report. *Grzybowski Foundation Special Publication* **13**, 57–61.
- Langezaal AM, Jannink NT, Pierson ES, van Der Zwan GJ (2005) Foraminiferal selectivity towards a bacteria: an experimental approach using a cell-permeant stain. *Journal of Sea Research* **54**, 256–275.
- Lee JJ (1980) Nutrition and physiology of the foraminifera. In *Biochemistry and Physiology of Protozoa* (eds Levandowsky M, Hunter SH). Academic Press, New York, pp. 43–66.
- Leoni L, Saitta M (1976) X-ray fluorescence analysis of 29 trace elements in rock and mineral standard. *Rendiconti della Società Italiana di Mineralogia e Petrologia* **32**, 497–510.
- Leoni L, Menichini M, Saitta M (1986) Determination of S, Cl, and F in silicate rocks by X-ray fluorescence analyses. *X-ray Spectrometry* **11**, 156–158.
- Lipps JH (1973) Test structure in foraminifera. *Annual Review Microbiology* **27**, 471–488.
- Lipps JH, Rozanov AY (1996) The late Precambrian-Cambrian agglutinated fossil Platysolenites. *Paleontological Journal* **30**, 679–687.
- Liu Q, Zhang Y, Laskowski JS (2000) The adsorption of polysaccharides onto mineral surfaces: an acid/base interaction. *International Journal of Mineral Processing* **60**, 229–245.
- Loeblich AR Jr, Tappan H (1987) *Foraminiferal Genera and their Classification*. Van Nostrand Reinhold Company, New York.
- Majewski W, Lecroq B, Sinniger F, Pawlowski J (2007) Monothalamous foraminifera from Admiralty Bay, King George Island, West Antarctica. *Polish Polar Research* **28**, 187–210.
- Makled WA, Langer MR (2010) Preferential selection of titanium-bearing minerals in agglutinated Foraminifera: ilmenite (FeTiO₃) in *Textularia hanerii* d'Orbigny from the Bazaruto Archipelago, Mozambique. *Revue de Micropaléontologie* **53**, 163–173.
- Maloof AC, Rose CV, Beach R, Samuels BM, Calmet CC, Erwin DE, Poirier GR, Yao N, Simons FJ (2010) Possible animal-body fossils in pre-Marinoan limestones from South Australia. *Nature Geosciences* **3**, 653–659.
- McIlroy D, Green OR, Brasier MD (2001) Paleobiology and evolution of the earliest agglutinated Foraminifera: Platysolenites, Spirosolenites and related forms. *Lethaia* **34**, 13–29.
- Nyholm KG (1957) Orientation and binding power of recent monothalamous foraminifera in soft sediments. *Micropaleontology* **3**, 75–76.
- Pawlowski J (2000) Introduction to the molecular systematics of foraminifera. *Micropaleontology* **46**, (Suppl. 1), 1–12.
- Pawlowski J, Majewski W (2011) Magnetite-bearing foraminifera from Admiralty Bay, West Antarctica, with description of *Psammophaga magnetica*, sp. nov. *Journal of Foraminiferal Research* **41**, 3–13.
- Pawlowski J, Holzmann M, Berney C, Fahrni J, Cedhagen T, Bowser SS (2002a) Phylogeny of allogromiid Foraminifera inferred from SSU rRNA gene sequences. *Journal of Foraminiferal Research* **32**, 334–343.
- Pawlowski J, Fahrni JF, Brykczynska U, Habura A, Bowser SS (2002b) Molecular data reveal high taxonomic diversity of allogromiid Foraminifera in Explorers Cove (McMurdo Sound, Antarctica). *Polar Biology* **25**, 96–105.
- Pawlowski J, Holzmann M, Berney C, Fahrni J, Gooday AJ, Cedhagen T, Habura A, Bowser SS (2003a) The evolution of early foraminifera. *Proceedings of the National Academy of Sciences USA* **100**, 11494–11498.
- Pawlowski J, Holzmann M, Berney C, Fahrni J, Cedhagen T, Bowser SS (2003b) Phylogeny of allogromiid foraminifera inferred from SSU rRNA gene sequences. *Journal of Foraminiferal Research* **32**, 334–343.
- Pawlowski J, Fahrni JF, Guiard Kathleen Conlan J, Hardecker J, Habura A, Bowser SS (2005) Allogromiid foraminifera and gromiids from under the Ross Ice Shelf: morphological and molecular diversity. *Polar Biology* **28**, 514–522.
- Pawlowski J, Holzmann M, Tyszk J (2013) New supraordinal classification of Foraminifera: molecules meet morphology. *Marine Micropaleontology* **100**, 1–10.
- Pigorini B (1968) Sources and dispersion of recent sediments of the Adriatic Sea. *Marine Geology* **6**, 187–229.
- Pike J, Kemp AES (1996) Silt aggregates in laminated marine sediment produced by agglutinated Foraminifera. *Journal of Sedimentary Research* **66**, 625–631.
- Roberts APD, Heslop XZ, Pike CR (2014) Understanding fine magnetic particle systems through use of first-order reversal curve diagrams. *Reviews of Geophysics* **52**, 557–602.
- Rothe N, Gooday AJ, Pearce RB (2011) Intracellular mineral grains in the xenophyophore *Nazareammmina tenera* (Rhizaria, Foraminifera) from the Nazare' Canyon (Portuguese margin, NE Atlantic). *Deep Sea Research I* **58**, 1189–1195.
- Sabbatini A, Bonatto S, Bianchelli S, Pusceddu A, Danovaro R, Negri A (2012) Foraminiferal assemblages and trophic state in coastal sediments of the Adriatic Sea. *Journal of Marine Systems* **105**, 163–174.
- Schieber J (2009) Discovery of agglutinated benthic foraminifera in Devonian black shales and their relevance for the redox state of ancient seas. *Palaeogeography, Palaeoclimatology, Palaeoecology* **271**, 292–300.
- Schieber J (2012) Styles of agglutination in benthic foraminifera from modern Santa Barbara Basin sediments and the implications of finding fossil analogs in Devonian and Mississippian black shales. In: *Anoxia: Evidence for Eukaryote Survival and Paleontological Strategies, Cellular Origin, Life in Extreme Habitats and Astrobiology 21* (eds Altenbach AV, Bernhard JM, Seckbach J). Springer, New York, pp. 573–589.
- Sever MJ, Weisser JT, Monahan J, Srinivasan S, Wilker JJ (2004) Metal-mediated cross-linking in the generation of a marine-mussel adhesive. *Angewandte Chemie International Edition* **43**, 448–450.
- Shepard FP (1954) Nomenclature based on sand-silt-clay ratios. *Journal of Sedimentary Petrology* **24**, 151–158.
- Spagnoli F, Dinelli E, Giordano P, Marcaccio M, Zaffagnini F, Frascari F (2014) Sedimentological, biogeochemical and mineralogical facies of Northern and Central Western Adriatic Sea. *Journal of Marine Systems* **139**, 183–203.
- Stamatakis A, Hoover P, Rougemont J (2008) A rapid bootstrap algorithm for the RAxML Web servers. *Systematic Biology* **57**, 758–771.
- Tamura K, Peterson N, Stecher G, Nei M, Kumar S (2011) MEGA5: molecular evolutionary genetics analysis using maximum likelihood, evolutionary distance, and maximum parsimony method. *Molecular Biology and Evolution* **28**, 2731–2739.
- Vasudevan D, Stone AT (1996) Adsorption of catechols, 2-aminophenols, and 1,2-phenylenediamines at the metal (Hydr)

- oxide–water interface: effect of ring substituents on the adsorption onto TiO₂. *Environmental Science and Technology* **30**, 1604–1613.
- Wang X, Lovlie R, Zhao X, Yang Z, Jiang F, Wang S (2010) Quantifying ultrafine pedogenic magnetic particles in Chinese loess by monitoring viscous decay of superparamagnetism. *Geochemistry Geophysics Geosystems* **11**, Q10008.
- Waskowska A (2014) Selective agglutination of tourmaline grains by foraminifera in a deep-water flysch environment (Eocene Hieroglyphic Beds, Silesian Nappe, Polish Outer Carpathians). *Geological Quarterly* **58**, 337–352.

SUPPORTING INFORMATION

Additional Supporting Information may be found in the online version of this article:

Fig. S1 Scanning Electron Microscope (SEM) micrographs were obtained using a ZEISS SUPRA 55 VP SEM with a third generation GEMINI field emission column, allowing a spatial image resolution down to 1.0 nm, in

scattered (SE) and backscattered (BSE) modes at the University of Paris VI-UMPC. SEM photographs of living *Psammophaga zirconia* specimens from the study area.

Fig. S2 SEM photographs and related EDS cartographies of living *Psammophaga zirconia* specimens (paratypes) from the study area.

Fig. S3 Magnetic properties of *Psammophaga zirconia* individuals.

Fig. S4 SEM photographs and related EDS cartographies of sediment samples <63 µm from the transect D.

Table S1 Summary of morphological features of measured intracellular mineral grains in four *Psammophaga zirconia* individuals.

Table S2 Grain-size data of sediment samples of the study area.

Table S3 Mineralogy, major and trace element data of sediment samples of the study area.